INL/CON-23-73061-Revision-0

Modeling of Prismatic High Temperature Reactors in Pronghorn

November 2023

Changing the World's Energy Future

Vasileios Kyriakopoulos, Mauricio Eduardo Tano Retamales, Sebastian Schunert

Idaho National Laboratory

INL/CON-23-73061-Revision-0

Modeling of Prismatic High Temperature Reactors in Pronghorn

Vasileios Kyriakopoulos, Mauricio Eduardo Tano Retamales, Sebastian Schunert

November 2023

Idaho National Laboratory
Idaho Falls, Idaho 83415

http://www.inl.gov

Prepared for the
U.S. Department of Energy
Under DOE Idaho Operations Office
Contract DE-AC07-05ID14517

Modeling of Prismatic High Temperature Reactors in Pronghorn

Vasileios Kyriakopoulos,* Mauricio Tano,* and Sebastian Schunert,*

*Computational Frameworks, Idaho National Laboratory, P.O. Box 2008, Idaho Falls,ID, vasileios.kyriakopoulos@inl.gov
mauricio.tanoretamales@inl.gov, sebastian.schunert@inl.gov

INTRODUCTION

Pronghorn is a MOOSE based thermal-hydraulics code developed at Idaho National Laboratory (INL) for advanced nuclear reactor analysis. It has been previously applied to model pebble-bed high temperature reactors (HTRs), liquid-metal cooled reactors, and molten salt reactors, among others. This work leverages the coarse-mesh modeling capabilities in Pronghorn to model the Oregon State University (OSU)'s High Temperature Test Facility (HTTF). The HTTF is a 1:4 height scaled-down facility of General Atomics' Modular High Temperature Gas-cooled Reactor (MHTGR). The facility is primarily built to generate data for code and model validation, and does not precisely replicate MHTGR conditions. Nevertheless, it encompasses the main physics associated with MHTGR transients.

The radial cross-section of the HTTF is shown in Figure 1. The core of the HTTF is composed of Greencast 94-F ceramic blocks in the inner reflector and graphite in the side reflector, similar to the MHTGR core configuration. It consists of a central reflector, heated core, and side reflector. The permanent reflector surrounding the ceramic blocks is made out of silicon carbide. Axially, the blocks are stacked upon one another and include the lower reflector, core, and upper reflector. The ceramic blocks contain 516 coolant channels (depicted in yellow) through which the helium coolant flows from top to bottom. Additionally, the central and side reflector, contain 6 and 36 coolant channels respectively (yellow circles), to mimic the bypass flow in a prototypical reactor. 210 graphite heating rods (depicted in red) are used to electrically heat the core. In this work, the rods are not individually modelled and heat is applied in the homogenized porous medium approach, directly deposited in the ceramic blocks.

A Pronghorn model is developed to calculate the steady state conditions of the HTTF, prior to the depressurised conduction cool-down (DCC) test initiation (test PG-26). Best-estimate boundary conditions are applied based on simulations previously performed with system codes [1].

THEORY

The flow within the prismatic-fueled HTR can be modeled using a porous media model. In the porous media representation, the gas and solid structures occupy the same space. The fluid volume fraction the porosity of the shared volume. In mathematical terms, the porosity can be defined as follows:

$$\gamma = \frac{V_f}{V_T}\,, \tag{1}$$

where V_f is the flow volume and V_T is the total volume. Prismatic assemblies are homogeneous in the axial direction (i.e., the geometry cross section is constant), and therefore

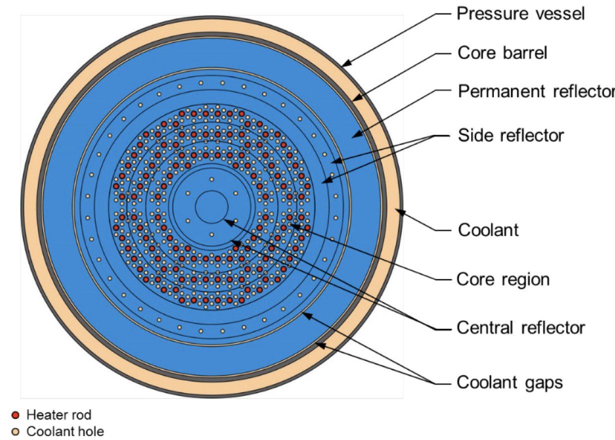

Fig. 1: Cross section of structures inside the reactor pressure vessel [1].

$\gamma = \frac{A_f}{A_T}$ with A_f being the area of the fluid flow and A_T the total area of the assembly.

Conservation equations for fluid mass, momentum, energy, and solid energy are coupled via momentum and energy exchanges between the phases. The porous flow equations for weakly-compressible flow are given by:

$$\frac{\partial \gamma\rho}{\partial t} + \nabla\cdot(\rho\boldsymbol{v}) = 0,$$
$$\frac{\partial \rho\boldsymbol{v}}{\partial t} + \nabla\cdot\left(\gamma^{-1}\rho\boldsymbol{v}\otimes\boldsymbol{v}\right) = -\gamma\nabla p + \gamma\rho\boldsymbol{g} - W\rho\boldsymbol{v}_I,$$
$$\frac{\partial \gamma\rho e}{\partial t} + \nabla\cdot(\rho H\boldsymbol{v}) - \nabla\cdot\left(\kappa_f\nabla T\right) + \alpha(T-T_s) = 0 \quad \text{on } \Omega_f$$
$$(1-\gamma)\rho_s c_{p,s}\frac{\partial T_s}{\partial t} - \nabla\cdot(\kappa_s\nabla T_s) - \alpha(T-T_s) = \dot{q}''' \quad \text{on } \Omega_s,$$

where $\boldsymbol{v}$ is the superficial velocity defined as $\boldsymbol{v} = \gamma\boldsymbol{v}_I$, with γ the porosity and $\boldsymbol{v}_I$ the interstitial or physical velocity, ρ is the density, p is the pressure, e is the internal energy, H is the enthalpy, T is the fluid temperature, T_s is the solid temperature, ρ_s is the solid density, $c_{p,s}$ is the specific heat of the solid phase, $\boldsymbol{g}$ is the gravity vector, W is the pressure drop coefficient, κ_f is the effective thermal conductivity of the fluid, α is the volumetric heat transfer coefficient between the fluid and the solid phase, κ_s is the effective solid thermal conductivity, and last $\dot{q}'''$ is the heat source in the solid (e.g., fission heat source). In porous medium modeling, the heat source is defined as the total power of the assembly, divided by the total volume. The effective thermal conductivity κ_f and κ_s are diagonal tensors.

The fluid domain Ω_f is comprised of porous regions with $0 < \gamma < 1$ and free flow regions with $\gamma = 1$; in the free-flow region, T_s is not solved, $\alpha = 0$, $W = 0$, and $\kappa_f = k_f$ (where k_f is the thermal conductivity of the fluid). Similarly, T_f is not solved in solid regions where $\gamma = 0$ and $\kappa_s = k_s$ with k_s the solid conductivity. $\kappa_{s,t}$ is the effective thermal conductivity of the solid in the transverse direction. Three different approaches are considered:

$$\kappa_{s,t} = \gamma k_f + (1-\gamma) k_s\,, \tag{2}$$

$$\kappa_{s,t} = \left(\frac{\gamma}{k_f} + \frac{1-\gamma}{k_s}\right)^{-1}\,. \tag{3}$$

and

$$\kappa_{s,t} = \sqrt{\gamma k_f (1-\gamma) k_s}. \tag{4}$$

MODEL OF THE HTTF

This section presents the Pronghorn model for OSU's HTTF. The model geometry is presented in Figure 2. The main flow components are the top plenum, top reflector, core, and bottom reflector. Radially, from interior to outside, the model contains the core (or upper/bottom reflector), the permanent reflector that extents from the top part of the upper reflector to the bottom part of the lower reflector, the helium gap, and core barrel. The flow is assumed to enter perpendicularly at the top face of the top plenum and to flow downwards to the lower plenum. The inlet temperature boundary condition is set to the temperature measured by the top plenum thermocouples of the HTTF.

A porous media model is used for the top/bottom reflectors and the heated core. Free flow conditions are assumed in the top plenum and the helium gap. Radiative heat conduction is modeled in the helium gap and solid heat conduction is modeled for all components except for the top plenum and the helium gap.

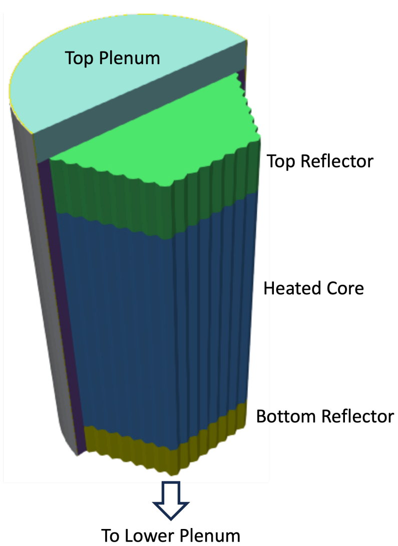

Fig. 2: Main flow components modeled in the HTTF.

The core reflectors (central/side) and heated core of the geometry are divided into hexagonal assemblies. There are 9 types of hexagonal assemblies. The cross section of the HTTF core and the adopted homogenization approach is shown in Figure 3. In this figure, cooling channels in the heated region are shown in yellow and heating rods are shown in red. All the heated rods have the same diameter, while the fuel coolant channels are divided into large cooling channels, placed within the heated section, and small and medium diameter cooling channels, which are placed in the boundaries of the heated section (inner and outer respectively). The cooling channels for the central and side reflector are shown in green.

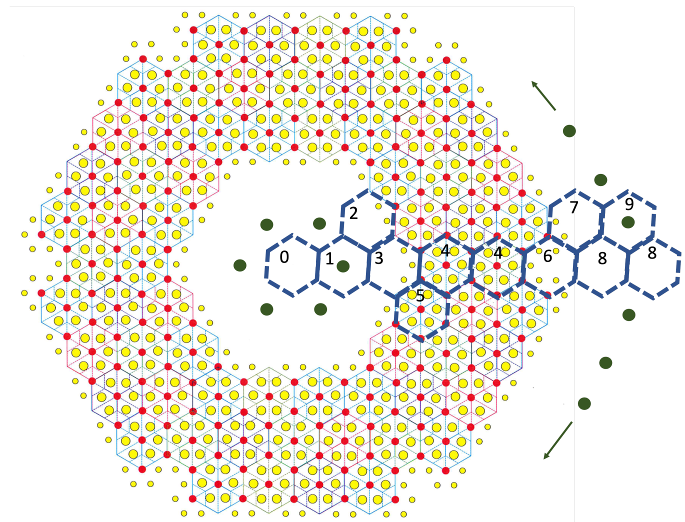

Fig. 3: Hexagonal homogenization of the core of the HTTF (adapted from HTTF blueprints).

The 9 hexagonal assemblies defined in this approach, are differentiated according to their unique heating power and effective flow area combination [2, 3]. Technically, there are only 8 distinct assembles since assemblies 0 and 8 shown in Figure 3 are equivalent. Nonetheless, in this model they are distinguished for the purpose of post-processing clarity, since the phenomena governing the temperature fields in those assemblies are very different. Assembly 0 is governed by heat conduction towards the center of the reactor, while assembly's 8 temperature field is regulated by long range heat diffusion from the heated region and cooling by the helium gap.

The characteristic parameters for each of the 9 hexagonal assemblies is detailed in Table I. In this table, the flow area, flow perimeter, total area, number of heating rods, and porosity of each assembly is specified. Note, the number of heating rods is used instead of the volumetric power per assembly, in order to be able to automatically adjust the power of the assembly during transient modeling. The composition of the core region of the HTTF is depicted in Figure 4. The core assemblies are grouped into inner (central) reflector, heated core, and outer (side) reflector. The power density is reported per homogenized fuel rod. This means that the actual power density of the assembly is determined by the product of the homogenized power density and the number of rods in the assembly.

TABLE I: Details of each of the homogenized assemblies for core blocks of the HTTF.

Index	**Flow Area (m^2)**	**Flow Perimeter (m)**	**Total Area (m^2)**	**Heating Rods**	**Porosity**
0	0	0	5.281e-3	0	-
1	4.909e-4	7.854e-2	5.281e-3	0	9.295e-2
2	1.571e-4	6.283e-2	5.281e-3	3.333e-1	2.975e-2
3	2.356e-4	9.425e-2	5.281e-3	6.667e-1	4.462e-2
4	1.206e-3	3.016e-1	5.281e-3	2	2.284e-1
5	1.206e-3	3.016e-1	5.281e-3	1.833	2.284e-1
6	6.637e-4	2.042e-1	5.281e-3	1.333	1.257e-1
7	2.655e-4	8.168e-2	5.281e-3	3.333e-1	5.027e-2
8	0	0	5.281e-3	0	-
9	2.011e-4	5.027e-2	5.281e-3	0	3.807e-2

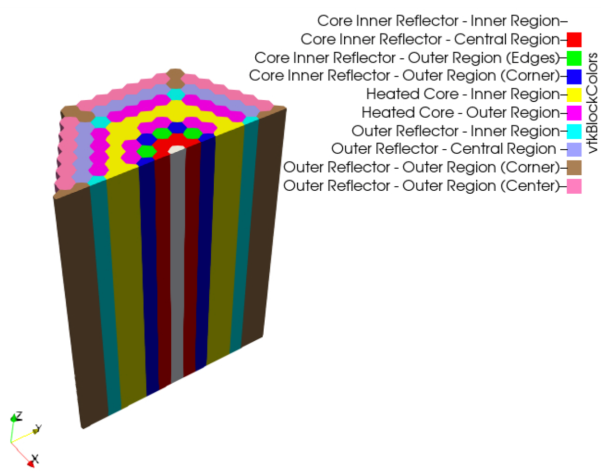

Fig. 4: Distribution of homogenized assemblies in the core region of the HTTF.

RESULTS AND ANALYSIS

The following boundary conditions are imposed for the best estimate steady state simulation of the HTTF: Inlet Fluid Temperature: 380K; Top Solid Fixed Temperature: 380K; Inlet Mass Flow Rate: $0.01\frac{kg}{s}$, Stagnant flow at the helium gap; Assembly Lateral Walls: No Slip and Conjugated Heat Transfer with the Solid; Core Barrel Wall: Free Convection with heat exchange coefficient $h = 10\frac{W}{m^2.K}$ and External Free Flow Temperature $T = 380$K; Outlet Fluid Temperature: Free Flow, Bottom Solid Temperature: Free Convection with Heat Exchange Coefficient $h = 10\frac{W}{m^2.K}$ and Free Convection Temperature equals to the Fluid Temperature at the Outlet; Outlet Pressure: 200×10^3Pa; Hydraulic Diameter for Fluid Flow: 0.01m, Porosity: 0.1831; Power Density per Homogenized Fuel Rod $13655.3\frac{W}{m^3}$.

Axial and radial cross-sections of the steady-state distribution of superficial velocity are depicted in Figure 5. The superficial velocity field shows larger flow cooling at the center of the heated region and the heated part of the core. The velocity has a negative sign because the coolant is flowing downwards.

The three methods for homogenizing the conductivity field in the solid (i.e., average (Eq 2), reciprocal (Eq. 3), and exponential (Eq. 4)) are compared using the temperature profiles obtained for each approach. The results for the fluid temperature fields are shown in Figure 6.

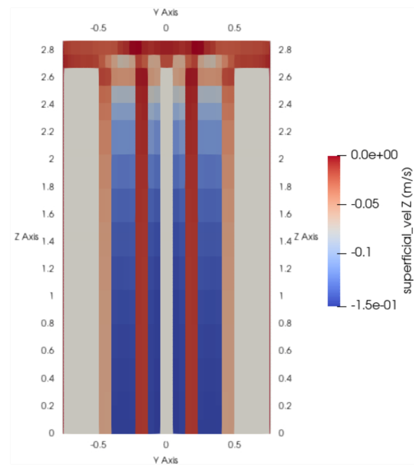

(a) Superficial Velocity - Axial Cut

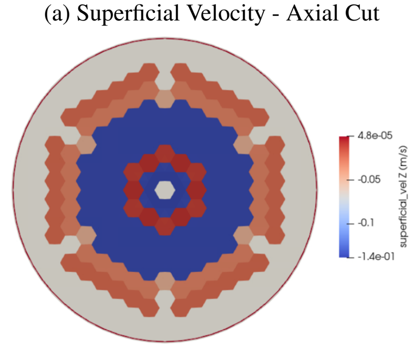

(b) Superficial Velocity - Radial Cut

Fig. 5: Results for the velocity field in the best-estimate steady-state boundary conditions for the HTTF.

The axial temperature profiles are consistent, with the maximum temperature rise occurring at the heated region of the core. However, the radial profiles differ. There is a significantly larger diffusion in the volume average approach that homogenizes the field in the radial direction. For the

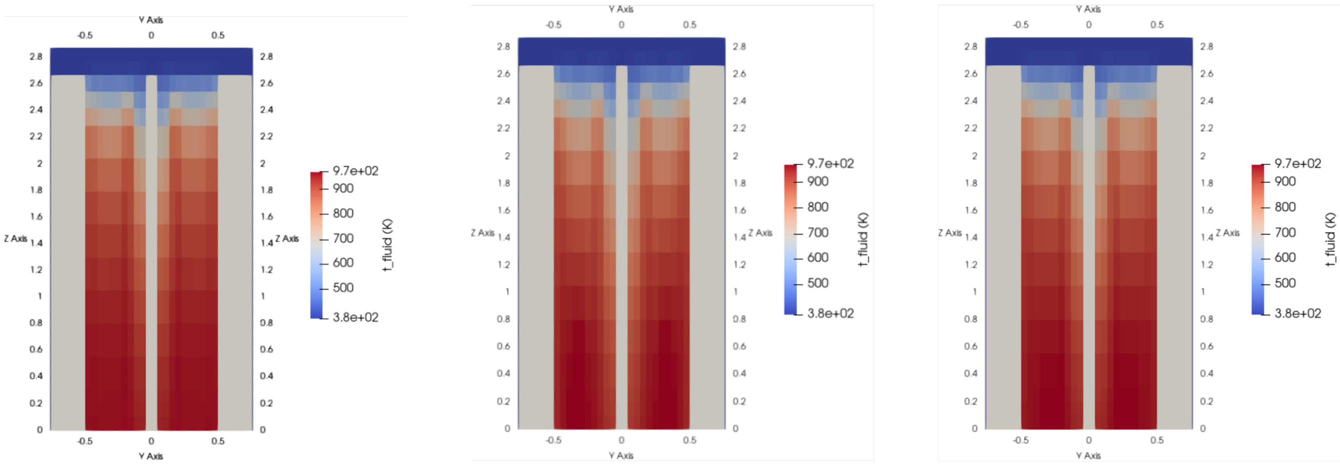

(a) Axial Cut - Volume Average

(b) Axial Cut - Reciprocal Average

(c) Axial Cut - Exponential Average

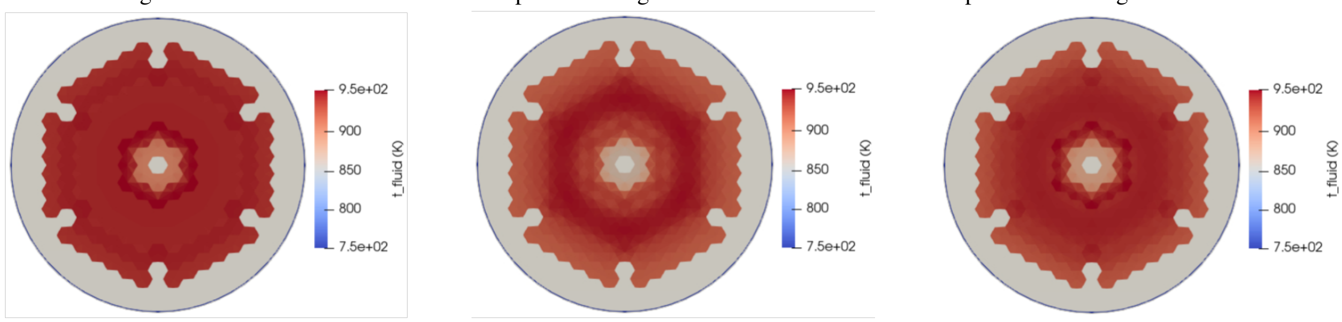

(d) Radial Cut - Volume Average

(e) Radial Cut - Reciprocal Average

(f) Radial Cut - Exponential Average

Fig. 6: Results for the **fluid** temperature profiles for different thermal conductivity homogenization approaches in the best-estimate steady-state model.

reciprocal average case, diffusion is limited and the heated core region is $\sim$ 100 K hotter than the inner and outer reflectors. Due to the mean squared average adopted for the coefficients of the exponential homogenization, the fluid temperature field distribution is not as skewed as the reciprocal average case, but it is less homogeneous than the volume average one.

CONCLUSIONS

In this work, the capabilities of Pronghorn to model the prismatic fuel HTR have been examined by developing a porous media flow model of OSU's HTTF. The lack of detailed experimental data on HTR's compelled the use of HTTF as a surrogate. This simulation demonstrates that the choice of conductivity modeling in the solid region has a significant effect on the temperature distribution in HTTF. Therefore, additional investigation into obtaining accurate averaged thermal properties is warranted.

The 3D porous media model developed has a few advantages when compared with the system codes' ring model to model the HTTF facility. First, it allows us to model asymmetric heating. Second, as 3D heat conduction is resolved, there is no need to adjust coefficients for the thermal conductivity. Finally, the homogenization of each assembly does not require the introduction of correction factors to convert the hexagonal shape to a ring geometry.

ACKNOWLEDGMENTS

This material is based upon work supported by a Department of Energy Nuclear Energy University Programs Graduate Fellowship.

REFERENCES

1. A. S. EPINEY, "RELAP5-3D Modeling of High Temperature Test Facility (HTTF) Test PG-26," Tech. rep., Idaho National Lab.(INL), Idaho Falls, ID (United States) (2020).
2. B. WOODS, "OSU High Temperature Test Facility Design Technical Report, Revision 2," (5 2019).
3. R. R. SCHULTZ, P. D. BAYLESS, R. W. JOHNSON, W. T. TAITANO, J. R. WOLF, and G. E. MCCREERY, "Studies related to the Oregon State University high temperature test facility: scaling, the validation matrix, and similarities to the modular high temperature gas-cooled reactor," Tech. rep., Idaho National Lab.(INL), Idaho Falls, ID (2010).